THE ASTROPHYSICAL JOURNAL, 543:L000–L000, 2000 November 1
© 2001. The American Astronomical Society. All rights reserved. Printed in U.S.A.

R AQUARII: CONSTRAINTS ON THE ROTATIONAL PERIOD OF THE LONG-PERIOD VARIABLE

J. M. HOLLIS,[1,2] J. A. PEDELTY,[3] J. R. FORSTER,[4] S. M. WHITE,[2] D. A. BOBOLTZ,[5] AND J. ALCOLEA[6]

Received 2000 May 2; accepted 2000 August 11; published 2000 October 6

ABSTRACT

We report Very Large Array (VLA) observations taken in 1996 November and 1998 May of the $v = 1$, $J = 1$–0, SiO maser line and BIMA array observations taken in 1999 December and 2000 February of the $v = 1$, $J = 2$–1, SiO maser line associated with the long-period variable (LPV) in the R Aquarii binary system that suggest rotation of the maser shell. From these interferometric data cubes, we determine that the maser shell rotation axis is approximately northeast-southwest, thus aligning approximately with the direction of the R Aqr jet; the sense of the maser shell rotation is such that northwest is approaching and southeast is receding; the period of rotation is ~17 yr. Alternatively, co-adding 72 time series spectra of the $v = 1$, $J = 1$–0, SiO maser line obtained during the period 1984 July–1990 May with a single-dish antenna, we constructed a composite spectral emission envelope that shows the LSR velocity limits of maser emission over this epoch. From this composite spectral emission envelope and Very Long Baseline Array observations in 1996 February of the $v = 1$, $J = 1$–0, SiO maser line, which show the maximal spatial extent of the maser shell, we obtain a shell rotation period of ~18 yr, which is in excellent agreement with the VLA and BIMA array results and represents the maximum rotation period of the LPV if corotating with the maser shell. On the other hand, we obtain a minimum rotation period for the LPV of ~5 yr if the LPV supplies material to the maser shell under the constraint of conservation of angular momentum. The ~5–18 yr range for the rotational period of the LPV determined here and the ~18 yr rotational period for the hot companion determined by previous investigators suggest that tidal effects at successive periastron passages in the R Aqr binary system are tending to synchronize these stellar rotational periods to the orbital period of ~44 yr.

Subject headings: circumstellar matter — masers — stars: individual (R Aquarii) — stars: rotation — stars: variables: other — techniques: interferometric

1. INTRODUCTION

R Aquarii is a symbiotic stellar system comprised of a mass-losing ~1–2 $M_\odot$ Mira-like long-period variable (LPV) with a 387 day period and a ~1.0 $M_\odot$ hot companion/accretion disk that is believed to give rise to the symmetrical jet seen at ultraviolet, optical, and radio wavelengths. The binary system orbit has been characterized as highly inclined to the line of sight ($i \sim 70°$) with large eccentricity ($e \sim 0.8$), a semimajor axis of $\sim 2.6 \times 10^{14}$ cm, and an orbital period of ~44 yr; it lies at a distance of 200 pc (see Hollis, Pedelty, & Lyon 1997 and references therein). Hence, the northeast-southwest–oriented jet probably undergoes episodic refueling and subsequent increased activity at periastron since the hot companion passes through the outer envelope of the LPV. It is further posited that the binary system was at apastron circa 1996 (Hollis et al. 1997), so the LPV envelope would be little influenced by either the jet or the hot companion/accretion disk for many years near this epoch.

Recently, Hollis & Koupelis (2000) developed a Lorentz force-driven parcel model for the R Aqr jet that depends on a strong stellar magnetic field of the rotating hot companion in the system; the model was constrained by disparate acceleration observed in the radio and ultraviolet manifestations of the jet and yielded an ~18 yr rotation period for the hot companion. Such a period is a sizable fraction of the orbital period, suggesting that the rotation periods of the two stars may tend to synchronize as a result of tidal interaction that is enhanced at periastron passage. Since the hot companion cannot be directly observed, presumably because of an occulting thick accretion disk seen nearly edge-on, and since maser emission is associated solely with the LPV, we conducted a study of SiO emission from recent interferometric array data (1996–2000) and time series spectra during the period 1984–1990 to determine the constraints on the rotational period of the LPV.

2. OBSERVATIONS

2.1. *Very Large Array Observations*

The R Aqr LPV was observed at 43 GHz with 12–13 antennas of the NRAO[7] Very Large Array (VLA) on 1996 November 19–20 and 1998 May 14. The antenna baselines ranged from 0.7 to 36 km, or, equivalently, from ~100 to 5150 kλ at a wavelength of 7 mm. The VLA correlator was operated in the 2AC spectral line mode with the on-line Hanning smooth option set and employed 64 spectral channels across a 3.125 MHz bandwidth centered on the $v = 1$, $J = 1$–0, SiO maser rest frequency of 43, 122.08 MHz, assuming the source velocity with respect to the local standard of rest ($V_{\rm lsr}$) is -26.0 km s^{-1}. This yielded a velocity resolution of 0.34 km s^{-1}. Each spectral line scan of R Aqr was 5 minutes in duration. One such scan (1996 November) and two such scans (1998 May) of R Aqr were made near transit. Contemporaneous 2 minute scans of

[1] Earth and Space Data Computing Division, Code 930, NASA Goddard Space Flight Center, Greenbelt, MD 20771.
[2] Department of Astronomy, University of Maryland, College Park, MD 20742.
[3] Biospheric Sciences Branch, Code 923, NASA Goddard Space Flight Center, Greenbelt, MD 20771.
[4] University of California, Berkeley, and Hat Creek Radio Observatory, 42231 Bidwell Road, Hat Creek, CA 96040.
[5] US Naval Observatory, 3450 Massachusetts Avenue, NW, Washington, DC 20392-5420.
[6] Observatorio Astronómico Nacional, Apartado 1143, E-2880 Alcalá de Henares, Spain.

[7] The National Radio Astronomy Observatory is operated by Associated Universities, Inc., under cooperative agreement with the National Science Foundation.

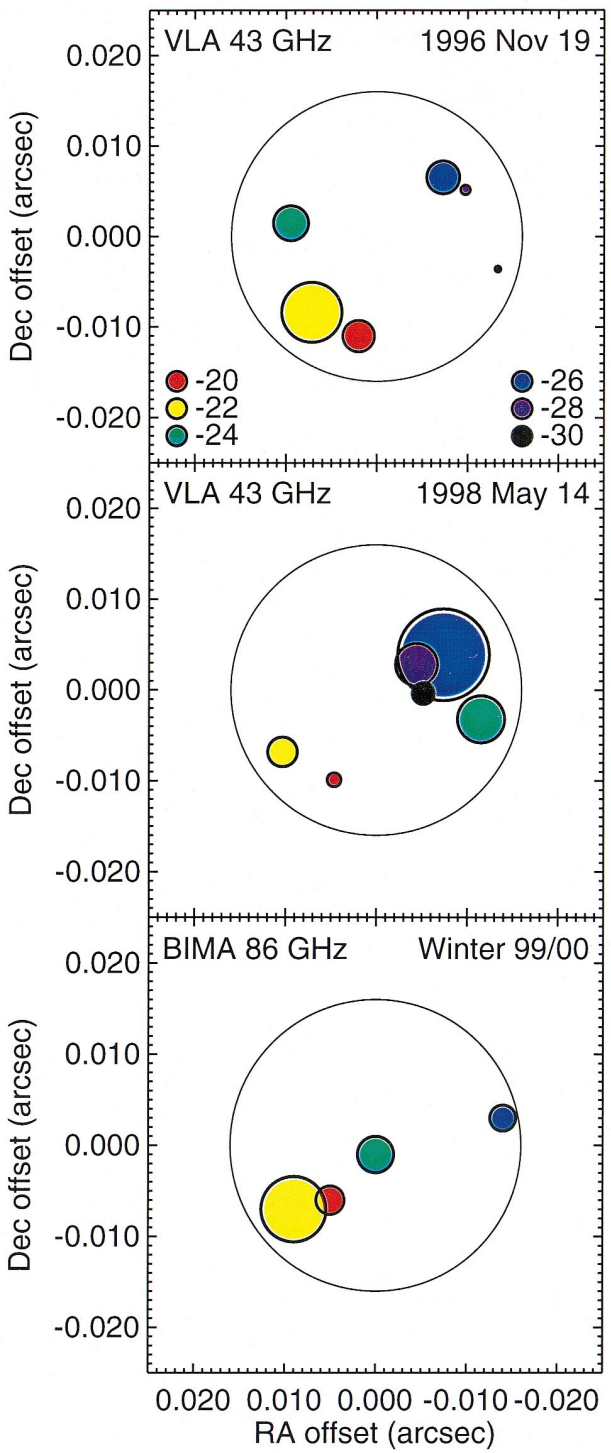

FIG. 1.—Locations of SiO maser features in VLA 43 GHz observations of the $v = 1$, $J = 1$–0 line and BIMA array 86 GHz observations of the $v = 1$, $J = 2$–1 line. Since in all cases the beamwidth in the images (50 mas at 43 GHz, 300 mas at 86 GHz) is much larger than the true size of the maser features, each circle represents the position of the centroid of emission integrated over a 2 km s^{-1} wide bandwidth (to achieve an acceptable signal-to-noise ratio) centered at the indicated velocity, with the diameter of the circle representing the strength of emission (using a square root scaling). The relative positions of features at different velocities at a given epoch are well determined, but the absolute positions at different epochs cannot reliably be determined, and the figures have been shifted so that the overall centroid is similar at each epoch. The 32 mas diameter circle shown for scale in each panel is approximately the maser shell diameter (see text). Uncertainties in the positions are generally smaller than 1 mas. In the bottom panel the -20 km s^{-1} circle represents an integration from -17 to -21 km s^{-1} in order to achieve sufficient signal-to-noise ratio. Uncertainties in the position fits range from 2 mas at -24 km s^{-1} to 0.5 mas at -22 km s^{-1}.

2348−165 were made to calibrate the spectral bandpass. Absolute flux calibration was achieved using our measured 1.48 Jy flux density for 2348−165 for the observational epochs. Standard spectral line processing techniques, including phase self-calibration using the "channel 0" data and CLEANing the individual channels, were used to produce a cube containing the spectrally resolved Stokes intensity SiO maser emission with a nominal spatial resolution of ~50 mas. Figures 1 and 2 show binned velocity ranges as a function of sky position and the spatially averaged maser profiles, respectively, from the resulting 1996 November and 1998 May VLA data cubes. The 1996 November and 1998 May epochs correspond, respectively, to minimum and maximum light for the LPV.

2.2. *BIMA Observations*

The R Aqr LPV was observed at 86 GHz with 10 antennas of the Berkeley-Illinois-Maryland Association (BIMA) array for short periods on 1999 December 19, 20, 26, and 29, 2000 January 1, 6, 18, 19, and 26, and 2000 February 2, 7, and 10. The BIMA array was in its most extended configuration, providing 45 interferometric baselines over the range 70–1700 m or, equivalently, 20–500 kλ at a wavelength of 3.4 mm. The correlator was configured to produce 256 channels over a 25 MHz lower sideband (LSB) bandwidth centered on the $v = 1, J = 2$–1, SiO maser line at a rest frequency of 86243.442 MHz, assuming the source $V_{\rm lsr}$ is -26.0 km s^{-1}. This yielded a velocity resolution of 0.34 km s^{-1}. The LSB channels of the combined data sets were self-calibrated in phase using an average of 30 channels centered on the peak of the maser emission. The time interval of the self-calibration was one integration period (11.5 s). Amplitude calibration was restricted to solving for relative antenna gain variations over a 10 minute interval after applying the phase calibration, using the amplitude of the maser emission as a reference. Figures 1 and 2 show binned velocity ranges as a function of sky position and the spatially averaged maser profiles, respectively, from the resulting BIMA array data cube. During these observations the LPV was near minimum light.

2.3. *CAY* 13.7 m *Observations*

The R Aqr LPV was monitored in the $v = 1, J = 1$–0, SiO maser during the period 1984 July to 1990 May with the 13.7 m antenna of the Centro Astronómico de Yebes (CAY) of the Spanish National Astronomical Observatory. The spectrometer used was a 256 channel filter bank with 50 kHz channel spacing, which is equivalent to a spacing of 0.35 km s^{-1} at 43 GHz. The characteristics of the telescope, the receivers used, and the calibration procedures to ensure valid comparison of measurements across this long observational epoch are detailed in Alcolea et al. (1999). An individual observation typically consisted of an hour long, frequency-switched scan with a total bandwidth of ~44 km s^{-1}. Scans were spaced at approximately 1 month intervals, resulting in a total of 72 spectra over the ~6 yr epoch. To construct a composite maser emission envelope that would show the total LSR velocity range of the maser emission of the LPV, we summed all 72 spectra and normalized the result to its highest peak as shown in the bottom panel of Figure 2.

3. DISCUSSION AND CONCLUSIONS

The conventional interpretation of the SiO maser profiles from cool supergiants, based on the very long baseline interferometry (VLBI) observations of a shell structure, is that they

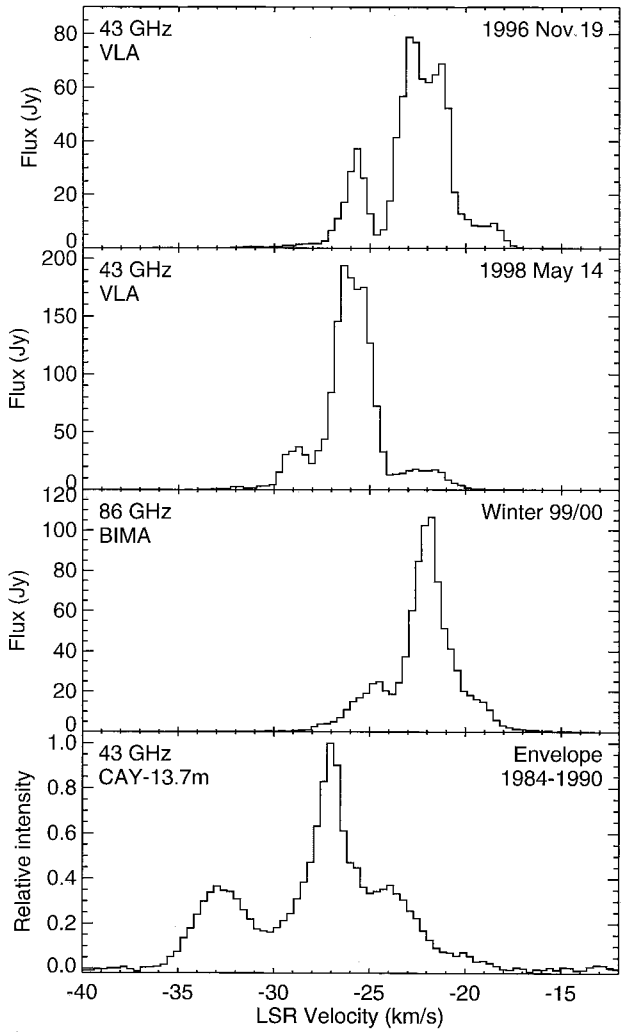

FIG. 2.—SiO maser spectral line profiles toward R Aqr. *Top two panels*: The $v = 1$, $J = 1$–0, SiO maser from VLA data of 1996 November and 1998 May. Each spectrum has a channel spacing of 48.828 kHz (~0.34 km s^{-1}). *Third panel*: The $v = 1$, $J = 2$–1, SiO maser from BIMA array data taken during the winter of 1999/2000. Channel spacing is 97.656 kHz (~0.34 km s^{-1}). *Bottom panel*: A summed, normalized composite of 72 $v = 1$, $J = 1$–0, SiO maser scans obtained with the CAY 13.7 m during the period from 1984 July to 1990 May. Channel spacing is 50 kHz (~0.35 km s^{-1}). Note that this panel shows one strong central peak, two satellite peaks of equal intensity, and the maximal LSR velocity extent of maser emission in the LPV envelope. The velocity midpoint between the two satellite peaks is consistent with the center of mass velocity of the LPV for this epoch. This work assumes the velocity difference between the two satellite peaks is a measure of the equatorial rotational velocity of the maser shell (see text). This panel is also intended to introduce the format of the movie (MPEG movie [~1.05 Mbytes]) presented in the electronic version showing the sequence of the 72 CAY spectra against a yellow background, which represents the composite single-dish spectrum. The movie shows that the highest peak in the CAY composite spectrum is predominantly due to an intense feature at a few epochs—it is not a persistent feature.

represent emission from just below the height in the stellar outflow where dust forms (and hence depletes Si in the outflow) along lines of sight tangential to a radial outflow where long coherent path lengths for maser amplification can be achieved. In any situation where maser amplification takes place, emission at a given frequency will be dominated by paths through the medium on which the line-of-sight velocity gradient is minimized. In a radial outflow this occurs for lines of sight tangential to the outflow, around the apparent limb of the star. If this is the case, the maser spots should show evidence of rotation in the atmosphere of the star, with the emission centered on the LSR velocity of the star (which will be the apparent velocity of gas flowing radially along the poles in the plane of the sky).

The pattern of emission in Figure 1 suggests that this is seen in the case of R Aqr. At three epochs over 4 years at two different frequencies, the two dominant velocity components (at -22 and -26 km s^{-1}) maintain the same spatial relationship to one another, and their separation is consistent with them being on opposite sides of the star. Conventionally, the fact that the line shapes change rapidly has been taken by most researchers to mean that the details of the maser profiles do not reflect a large-scale velocity pattern (see Elitzur 1992, p. 282) but rather just random motions in the atmosphere that happen to produce long amplification paths at certain velocities for brief periods. For example, large convection cells are believed to occur in red supergiants, and these will induce nonradial velocities that may appear as line-of-sight velocity shifts at the limb and may even produce occasional lines of sight toward the stellar disk that have sufficient amplification path length to produce an observable feature. However, in such an interpretation it is not clear how two components that change in strength considerably over the 4 years (e.g., BIMA array observations in 1998 March show very little emission at -22 km s^{-1}, and Gray et al. 1997 show major changes over 18 months) could recur at the same relative locations unless there is an organized large-scale velocity pattern.

Reprocessing of Very Long Baseline Array (VLBA) data at a resolution similar to that of the VLA data in Figure 1 did not show any appreciable velocity gradient across the maser shell, and in particular the maser emission is confined to radii larger than we infer from the VLA and BIMA data. However, the VLBA data suffer from a "missing flux" problem: the SiO emission is spread over a dimension of order 40 mas, but the VLBA data are not sensitive to sources larger than a few milliarcseconds. Hence, the VLBA images severely undersample any large-scale emission present and may resolve out any spots larger than a few milliarcseconds. This problem of missing VLBI flux has been demonstrated for SiO maser emission from VX Sgr (see Fig. 5 of Doeleman, Lonsdale, & Greenhill 1998). The shell size inferred from the VLBA images is larger than implied by the BIMA array and VLA data; this may be due to the fact that the VLBA is only sensitive to emission on small spatial scales, and the bright compact features in the VLBA images may occur at the outer edge of the maser shell, where theory predicts coherent path lengths will be maximized, while the larger beams of the VLA and BIMA array sample smoother emission closer to the star. It might be argued that because the VLA and BIMA array maps at a given velocity may include emission from both sides of the shell along the line of sight, the centroids for a given velocity will always lie between any different contributing components and thus lie at a smaller projected radius, but when we convolve the VLBA images to the VLA resolution we do not find that this is a significant effect at most velocities; it may be affecting the position of the -24 km s^{-1} component in the VLA and BIMA array data. We note also that the 43 GHz spectrum on the shortest VLBA baseline differs from the 86 GHz spectrum observed at the Swedish-ESO Submillimeter Telescope (SEST) in 1995 December and 1996 February by showing no emission at -30 km s^{-1}, although the spectra at the different frequencies appear similar in 1995 June and 1996 April (Gray et al. 1997; Boboltz, Diamond, & Kemball 1997). Similarly, the 43 GHz

VLA spectrum in 1996 November has the −22 and −26 km s^{-1} components at relatively different strengths than the SEST 86 GHz data show.

If indeed the spatial offset between the −22 and −26 km s^{-1} components represents rotation, then the maser shell may be rotating about a northeast-southwest axis, which is consistent with the assumption that the observed R Aqr jet, which also lies on such an axis, flows along the poles of the binary system (which assumes that the rotational axes of the two stars are aligned from angular momentum considerations). We can estimate a maser shell rotation period $P_{\rm MS}$ from corresponding spatial and spectral data from Figures 1 and 2, respectively, using the formula

$$P_{\rm MS} = \pi D_{\rm MS}/V_{\rm MS}, \quad (1)$$

where $D_{\rm MS}$ is the diameter of the maser shell and $V_{\rm MS}$ is the rotation rate of the maser shell. The VLA and BIMA array data at all three epochs in Figure 2 show a similar velocity difference of ∼8 km s^{-1}, which is the foreshortened result of $\Delta V \sin i$. Since the inclination angle of the R Aqr orbital axis is $i \sim 70°$ (Hollis et al. 1997), presumably the rotational axis of the maser shell would have a similar inclination. For maser shell rotation, $V_{\rm MS} = \Delta V/2 \sim 3.75$ km s^{-1}. According to Figure 1, $D_{\rm MS} \sim 22$ mas $= 6.4 \times 10^{13}$ cm at a distance of 200 pc (Hollis et al. 1997), and, using equation (1), we obtain $P_{\rm MS} \sim$ 17 yr.

Since Figure 1 clearly suggests maser shell rotation, we explore another way to validate the rotation period. Because the maser shell rotation axis is suitably placed (i.e., nearly in the plane of the sky), one could determine the shell rotation period were it not for the unpredictable nature of the maser emission itself. Features come and go in an apparently random fashion (e.g., see Fig. 7 of Alcolea et al. 1999), but all features are constrained by a composite emission envelope that could be deduced if enough time series data were available. Hence, this is the reason for summing all 72 CAY spectra in the case of R Aqr (Fig. 2, *bottom panel*). Notice in this figure that there are three peaks, a strong central one at ∼−27.5 km s^{-1} and two satellite peaks of equal intensity on either side of the central peak. The central peak is not a persistent feature as shown in the movie (see Fig. 2 caption) as well as Figure 7 of Alcolea et al. (1999). The midpoint velocity between the two satellite peaks is consistent with the center of mass velocity of the LPV near the epoch of these observations (see Hinkle et al. 1989). We use the two satellite peaks as an indication of the velocity extrema for our analysis. The velocity difference between the satellite peaks is $\Delta V \sin 70° \sim 9.1$ km s^{-1} and, therefore, $V_{\rm MS} = 4.84$ km s^{-1}. From VLBA observations (Boboltz et al. 1997), the maximal maser shell diameter $D_{\rm MS} \sim 31$ mas $= 9 \times 10^{13}$ cm at 200 pc (Hollis et al. 1997). Note that the VLBA senses small-scale structure and sharp gradients in the maser shell, and the shell radius inferred from the VLBA images should be representative of the maser shell radius as long as the thickness of the shell is small compared to its diameter. Thus, the VLBA data, which represent the maximum spatial extent of maser emission, and the CAY data shown in the bottom panel of Figure 2, which represent the maximum velocity extent of maser emission, yield $P_{\rm MS} = 18.5$ yr, a value in good agreement with that obtained previously from the VLA and BIMA array data. The rotational period of the maser shell could be in corotation with the LPV rotational period, and therefore we consider an ∼18 yr period an estimate of the maximum rotational period that the LPV can have.

We can obtain an estimate of the minimum LPV rotational period from angular momentum considerations. Since the maser shell must have been supplied material from the mass-losing LPV, any material flowing from the photosphere to the shell will be constrained by conservation of angular momentum (i.e., $V_{\rm MS} R_{\rm MS} = V_* R_*$). From IR observations, van Belle et al. (1996) obtain 16.1 mas for the angular diameter of the LPV in the R Aqr binary system, which, in turn, yields an LPV radius of 336 $R_\odot$ at 200 pc. Thus, conservation of angular momentum implies that the equatorial velocity V_* of the LPV is 9.3 km s^{-1}, which, in turn, implies that the rotational period of the LPV is ∼5.0 yr. An equatorial rotational velocity of 9.3 km s^{-1} for the LPV in R Aqr is consistent with the equatorial rotational velocity of 9.0 km s^{-1} as determined for the slightly more massive M giant in the symbiotic system BX Mon (Dumm et al. 1998) and the equatorial rotational velocity of $\sim 13(\sin i)^{-1}$ km s^{-1} as determined for the M supergiant VX Sgr (Doeleman et al. 1998).

In conclusion, Figure 1 suggests that the maser shell rotation axis is approximately northeast-southwest, thus aligning approximately with the direction of the R Aqr jet; the maser shell rotation is such that northwest is approaching and southeast is receding, and our analysis provides a ∼5–18 yr range for the rotational period of the LPV. This range for the LPV rotational period, combined with an ∼18 yr rotational period for the hot companion (Hollis & Koupelis 2000), suggests that tidal effects at successive periastron passages in the R Aqr binary system are tending to synchronize these stellar rotational periods to the orbital period of ∼44 yr (Hollis et al. 1997). The results and analysis herein may prove useful for constraining rotational periods of other SiO maser-emitting LPVs with rotational axes highly inclined to the line of sight.

We thank the two referees for suggestions that improved the presentation of this work. J. M. H. gratefully acknowledges the hospitality of the University of Maryland, College Park, where he was a sabbatical visitor during the course of this study. J. M. H. and J. A. P. received support from NASA RTOP 344-02-03-01. The use of BIMA for scientific research is supported by NSF grants AST 96-13998 to the University of California at Berkeley and AST 96-13716 to the University of Maryland.

REFERENCES

Alcolea, J., et al. 1999, A&AS, 139, 461
Boboltz, D. A., Diamond, P. J., & Kemball, A. J. 1997, ApJ, 487, L147
Doeleman, S. S., Lonsdale, C. J., & Greenhill, L. J. 1998, ApJ, 494, 400
Dumm, T., Mürset, U., Nussbaumer, H., Schild, H., Schmid, H. M., Schmutz, W., & Shore, S. N. 1998, A&A, 336, 637
Elitzur, M. 1992, Astronomical Masers (Dordrecht: Kluwer)
Gray, M. D., Ivison, R. J., Humphreys, E. M. L., & Yates, J. A. 1997, MNRAS, 295, 970
Hinkle, K. H., Wilson, T. D., Scharlach, W. W. G., & Fekel, F. C. 1989, AJ, 98, 1820
Hollis, J. M., & Koupelis, T. 2000, ApJ, 528, 418
Hollis, J. M., Pedelty, J. A., & Lyon, R. G. 1997, ApJ, 482, L85
van Belle, G. T., Dyck, H. M., Benson, J. A., & Lacasse, M. G. 1996, AJ, 112, 2147